

## Photoluminescence study of oxidation-induced faults in 4H-SiC epilayers

Yutaro Miyano, Ryosuke Asafuji, Shuhei Yagi, Yasuto Hijikata, and Hiroyuki Yaguchi

Citation: *AIP Advances* **5**, 127116 (2015); doi: 10.1063/1.4938126

View online: <http://dx.doi.org/10.1063/1.4938126>

View Table of Contents: <http://scitation.aip.org/content/aip/journal/adva/5/12?ver=pdfcov>

Published by the *AIP Publishing*

---

### Articles you may be interested in

[Application of UV photoluminescence imaging spectroscopy for stacking faults identification on thick, lightly n-type doped, 4°-off 4H-SiC epilayers](#)

*AIP Advances* **5**, 037121 (2015); 10.1063/1.4915128

[Observation of stacking faults from basal plane dislocations in highly doped 4H-SiC epilayers](#)

*Appl. Phys. Lett.* **100**, 042102 (2012); 10.1063/1.3679609

[Nonradiative recombination at threading dislocations in 4H-SiC epilayers studied by micro-photoluminescence mapping](#)

*J. Appl. Phys.* **110**, 033525 (2011); 10.1063/1.3622336

[Structural analysis and reduction of in-grown stacking faults in 4H-SiC epilayers](#)

*Appl. Phys. Lett.* **86**, 202108 (2005); 10.1063/1.1927274

[Stacking fault formation in highly doped 4H-SiC epilayers during annealing](#)

*Appl. Phys. Lett.* **81**, 3759 (2002); 10.1063/1.1519961

---

Searching? Trust *CiSE*.

It's peer-reviewed and appears in the IEEE Xplore and AIP library packages.

## Photoluminescence study of oxidation-induced faults in 4H-SiC epilayers

Yutaro Miyano, Ryosuke Asafuji, Shuhei Yagi, Yasuto Hijikata,<sup>a</sup>  
and Hiroyuki Yaguchi

*Division of Mathematics Electronics and information Sciences, Graduate School of Science and Engineering, Saitama University, 255 Shimo-Okubo, Sakura-ku, Saitama 338-8570, Japan*

(Received 16 June 2015; accepted 4 December 2015; published online 14 December 2015)

We investigated the effect of thermal oxidation on crystalline faults in 4H-SiC epilayers using photoluminescence imaging. We found that a comb-shaped dislocation array was deformed by thermal oxidation. We also found that line-shaped faults perpendicular to the off-cut direction were formed during oxidation and were stretched and increased with the oxidation time. Since these line-shaped faults were peculiar to the oxidation and stretched/increased with the oxide growth, they were identified as oxidation-induced stacking faults as seen in Si oxidation. © 2015 Author(s). All article content, except where otherwise noted, is licensed under a Creative Commons Attribution 3.0 Unported License. [<http://dx.doi.org/10.1063/1.4938126>]

Silicon carbide (SiC) semiconductors are attractive for the development of high-power, high-temperature, and high-frequency devices, due to their superior physical properties.<sup>1</sup> However, stacking faults (SFs) and dislocations are easily incorporated in SiC epitaxial layers,<sup>2-5</sup> which may cause severe degradation of the SiC power device performance.<sup>6-10</sup> Thermal oxidation processes are often used in the fabrication of SiC devices because SiO<sub>2</sub> film grown by thermal oxidation is utilized as a metal-oxide-semiconductor (MOS) junction or a surface passivation film. However, it has been reported that the quality of the SiC layer just under the SiO<sub>2</sub> film changes after thermal oxidation. For example, Hiyoshi and Kimoto reported that carbon vacancies present in an as-grown epilayer are filled with carbon interstitials that diffuse to the SiC layer during thermal oxidation.<sup>11</sup> On the other hand, Okojie *et al.*<sup>12</sup> reported that the thermal oxidation of highly doped (10<sup>19</sup> cm<sup>-3</sup> order) 4H-SiC epilayers induces the formation of multiple SFs with the 3C structure. We have previously investigated the effect of thermal oxidation on SFs in a 4H-SiC epitaxial layer using micro-photoluminescence (micro-PL),<sup>13</sup> where the formation/expansion of SFs (emission wavelength: 425.5 nm) was found to be caused by thermal oxidation. However, because the micro-focusing excitation laser beam used in micro-PL expands the SFs in a wide and complex way, detailed observation of the SFs cannot be performed. In this study, we have investigated the effect of thermal oxidation on SFs using PL imaging, where the power density and irradiation time of the excitation laser light were significantly reduced, and dislocations could also be observed from near-infrared-band emissions.<sup>14</sup>

Commercial *n*-type 4H-SiC (0001) substrates with a carrier concentration of 1 × 10<sup>16</sup> cm<sup>-3</sup>, an 8° off-orientation towards [11-20], and an epilayer thickness of 10 μm were used. A He-Cd laser (λ = 325 nm) was used as the excitation source for PL imaging measurements. PL images were magnified with objective lens and captured by a CCD camera through a long-pass optical filter (>700 nm) or a band-pass optical filter (438±12 nm). PL imaging was firstly performed at room temperature to observe the comb-shaped basal plane dislocation (BPD) array along the [1-100] direction, which was taken up in our previous work.<sup>13,15</sup> Prior to oxidation of the sample, laser irradiation in the vicinity of the comb-shaped BPD array was performed and PL images obtained before and after laser irradiation were compared. A Q-switched ultraviolet laser (λ = 266 nm) with a spot diameter of 0.7 μm and an irradiation power of 160 μW (power density *ca.* 4 × 10<sup>4</sup> W/cm<sup>2</sup>) was used as an irradiation source.

<sup>a</sup>E-mail: [yasuto@opt.ees.saitama-u.ac.jp](mailto:yasuto@opt.ees.saitama-u.ac.jp)



Annealing in Ar was then conducted at 1000 °C for 1 h, followed by thermal oxidation at 1100 °C in a dry oxygen flow of 1 slm for 10 h. The effect of thermal oxidation for a sample without laser irradiation was also investigated. In this case, thermal oxidation was performed at 1100 °C in a dry oxygen flow of 1 slm for 5 h, followed by 5 h, 12 h and 10 h oxidations with same condition. PL images were observed before and after each thermal oxidation step. After the third and fourth oxidation steps, laser irradiation was performed. A He-Cd laser ( $\lambda = 325$  nm) with an irradiation power of 3.66 mW (power density *ca.*  $3 \times 10^{-2}$  W/cm<sup>2</sup>) was used as an irradiation source.

Figure 1 shows PL images (a) before and (b) after laser irradiation, and (c) after Ar annealing. SFs were formed on both sides of the comb-shaped BPD array by laser irradiation. Only SFs formed by laser irradiation then disappeared after Ar annealing. These new SFs are very similar to the trapezoidal defects reported by Berechman *et al.* and considered to be single Shockley SFs (1SSFs) because the emission wavelength of these SFs is approximately 426 nm and they can be easily removed by annealing.<sup>16</sup> We pointed out that this irradiation-induced SF near the comb-shaped BPD array was vanished by oxidation.<sup>13</sup> However, the key for the vanish is not oxidation but thermal treatment. Cross-sectional transmittance electron microscopy confirmed that the stacking sequence in the vicinity of the comb-shaped BPD array was (3,1) in Zhdanov's notation (not shown here). Therefore, these SFs are identified as 1SSFs.<sup>4</sup>

Figure 2 shows the PL images of the sample after thermal oxidation. The BPD was found to be deformed toward the [1-100] or [-1100] direction by thermal oxidation. Although it has been known that such a BPD often moves or is changed in length by current injection or thermal treatment, to our knowledge, the deformation like a bow is unable to occur except the oxidation. This shows the intense interface strain due to the oxidation.

Both the irradiation-induced SFs (i.e. trapezoidal defects) and the SFs in the vicinity of the comb-shaped BPD array were 1SSFs. According to the report by Miyanagi *et al.*,<sup>17</sup> there are two types of 1SSF; isosceles triangle (looped basal-plane dislocation; BPD) and right-angled triangle

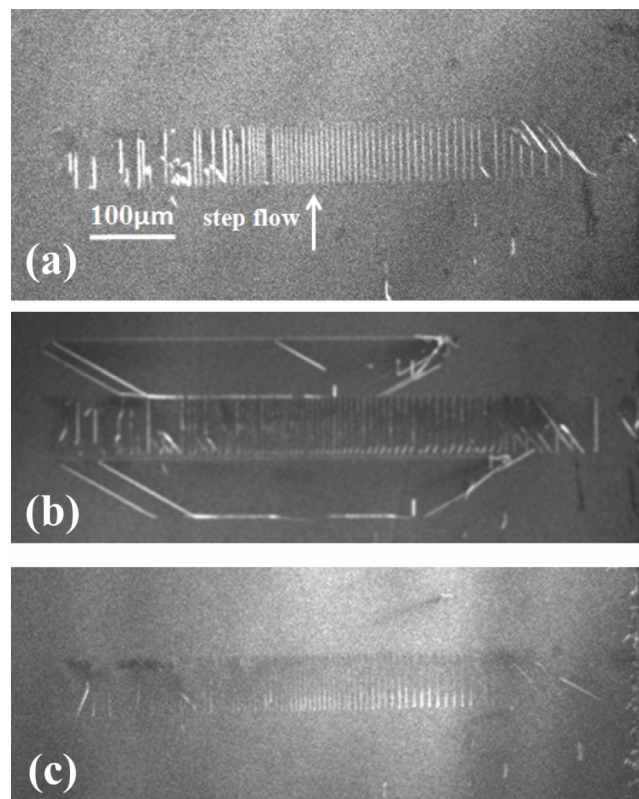


FIG. 1. PL image obtained with a long-pass filter ( $>700$  nm) (a) before and (b) after irradiation, and (c) after Ar annealing.

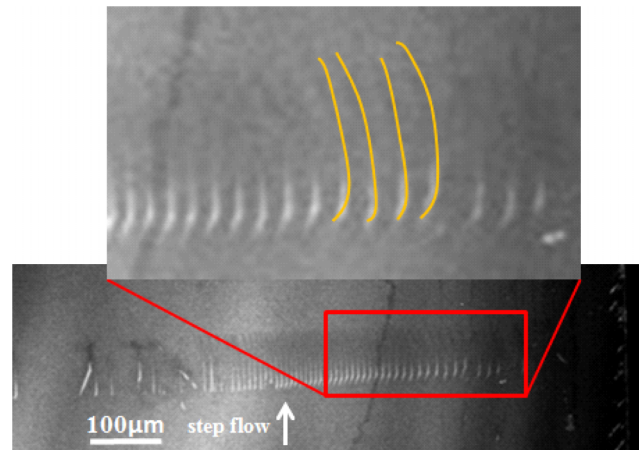


FIG. 2. PL image obtained with a long-pass filter ( $>700$  nm) after thermal oxidation.

(propagated BPD). They also reported that the looped-type 1SSF shrinks and vanishes easily by annealing, whereas the propagated-type 1SSF is difficult to shrink. Therefore, we consider that the SFs expanded by laser irradiation are looped-type 1SSFs and the SFs deformed by thermal oxidation are propagated-type 1SSFs.

Figure 3 shows PL images of a sample through a band-pass filter ( $438 \pm 12$  nm) (a) before and (b) after 10 h oxidation, (c) after 22 h oxidation, and (d) after 32 h oxidation. Line-shaped faults were observed perpendicular to the off-cut direction formed after 10 h oxidation (indicated by white solid arrows in Fig. 3(b)), and these faults were extended after the second and third oxidation steps. For the

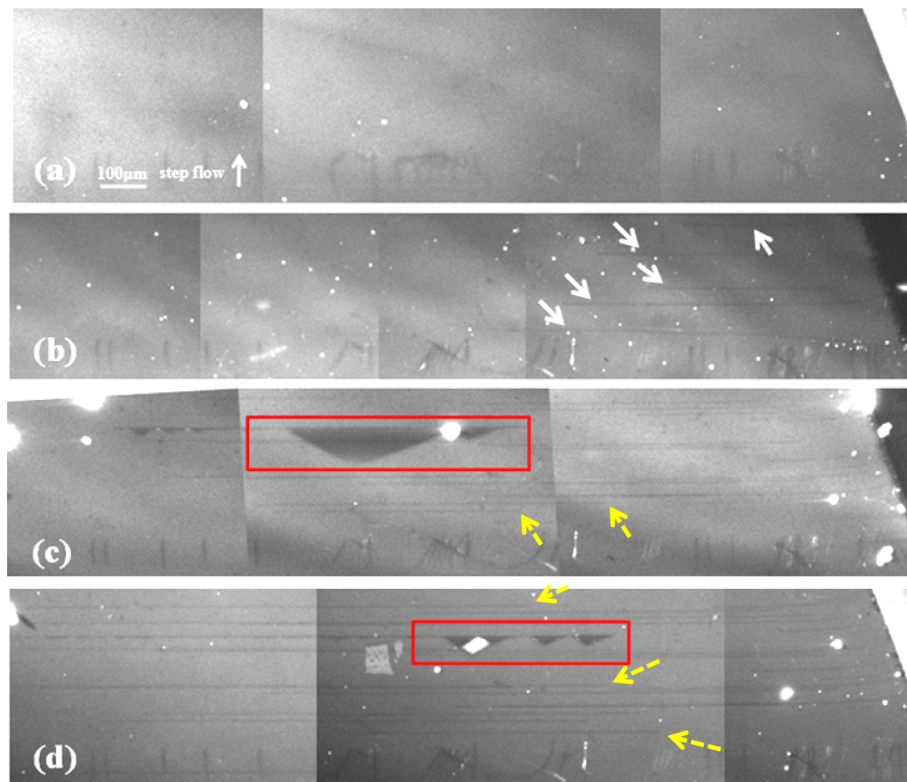


FIG. 3. PL image obtained with a band-pass filter ( $438 \pm 12$  nm) (a) before oxidation, (b) after 10 h oxidation, (c) after 22 h oxidation, and (d) after 32 h oxidation. The arrows denote the line-shaped faults including the faults formed inside the sample (shown by yellow dashed arrows).

reference, Ar anneal with same temperature as the oxidation for 10 h was carried out. As a result, no line-shaped fault was formed. Therefore, this line-shaped fault is induced not by thermal treatment but by oxidation. These faults are not observed through the long-pass optical filter ( $>700$  nm); therefore, they may not be dislocations because any type of dislocations have near-IR emissions.<sup>14</sup> The triangular SFs shown in Fig. 3(c) (inside the red rectangle) were formed by laser irradiation and expanded from the line-shaped faults along the off-cut direction, in addition to getting wider with the irradiation time. However, the expansion of this SF stopped when its height reached the length that corresponds to the thickness of epilayer. These SFs shrunk after the third oxidation, but were re-expanded by laser irradiation (inside the red rectangle of Fig. 3(d)). From the direction of expansion and maximum height of SF, they extend from the oxidizing interface to the epilayer/substrate interface. Although all the line-shaped faults appear to form from the edge of wafer, there are some faults that form inside the substrate. For example, the line-shaped faults pointed by yellow dashed arrows in Fig. 3(c) and 3(d) are such correspondences. In addition, the line-shaped faults were also confirmed from around the center of wafer (not shown here). Therefore, the line-shaped fault is not a fault peculiar to the edge of wafer or sample.

Figure 4 shows the PL spectrum emitted from the triangle-shaped SFs. These SFs are considered to be double Shockley SFs (2SSFs)<sup>18,19</sup> because of their emission wavelength (500 nm).<sup>4</sup> Maximenko and Sudarshan<sup>20</sup> also reported triangle-shaped 2SSFs that extend from nucleation sites near the epitaxial layer surface. However, since the shape of the nucleation site is much different from that of the line-shaped fault, these faults should not be the same kind. As mentioned above, the line-shaped faults were extended with increasing oxidation time, therefore, they should be a kind of SFs perpendicular to the direction of step flow. Since we observed from the side of the SFs, its shape was regarded as a line.

Figure 5 shows the oxidation time dependence of the line-shaped fault density and the average length of line-shaped faults. The blue line in the figure denotes the line fitted to the observed values after 600 min growth. The density increases linearly after an oxidation time of approximately 400 min, which implies that the formation of line-shaped faults has a threshold in the oxidation time or oxide thickness. This threshold time corresponds to an oxide thickness of 34 nm, which is almost equal to that at which the oxidation rate levels down,<sup>21</sup> i.e., the accumulation of Si interstitials in the oxide becomes saturated.<sup>22</sup> According to the report on Si oxidation by Taniguchi *et al.*,<sup>23</sup> when the oxide growth rate is sufficiently low, the concentration of Si interstitials in the oxide is fixed at the equilibrium concentration, and the Si interstitials predominantly diffuse into the Si substrate. In general, when the Si emission into the substrate due to oxidation is enhanced and the Si interstitials are accumulated near the oxidizing interface, an extrinsic stacking fault, termed oxidation-induced stacking fault (OSF), is formed,<sup>24</sup> as shown in Fig. 6. Therefore, the line-shaped fault is considered to be an

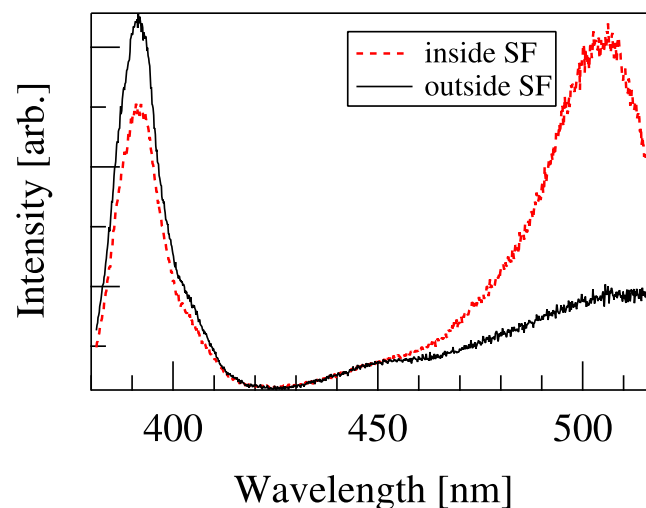


FIG. 4. PL spectra obtained from inside and outside the triangle-shaped SF.

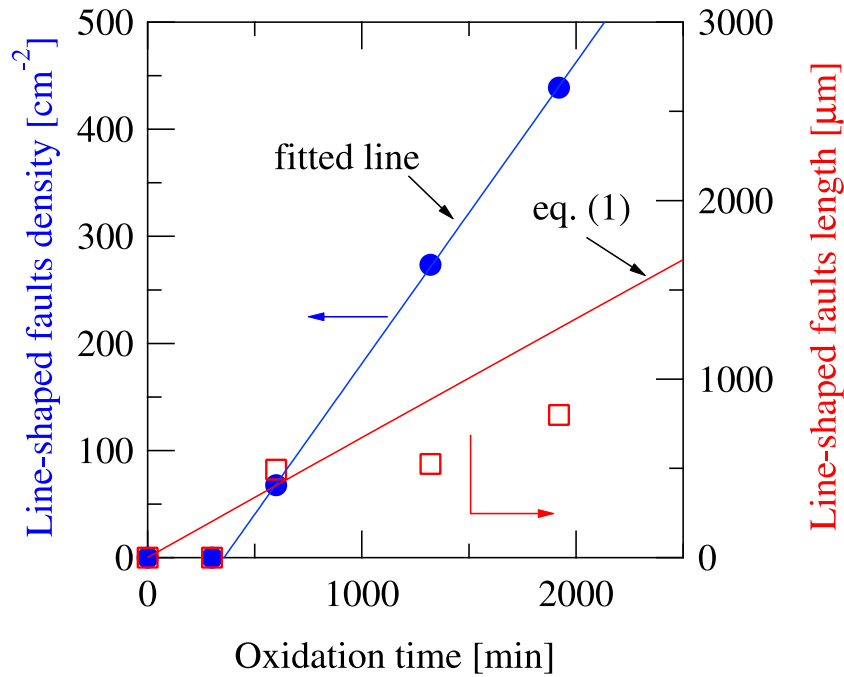


FIG. 5. Line-shaped fault density and average length of line-shaped faults as a function of oxidation time.

OSF because it should be formed by the accumulation of Si interstitials in the SiC substrate during oxidation, similarly to the case of OSF for Si.<sup>24</sup>

In the case of Si oxidation, the length of OSFs,  $l$ , is expressed with the oxide growth rate ( $dX/dt$ ):<sup>24</sup>

$$l = \frac{RK_1 \left(\frac{dX}{dt}\right)t}{\left(1 + K_2 \left(\frac{dX}{dt}\right)\right)^{\frac{1}{2}} - 1} - RC_1^f t, \tag{1}$$

where  $R$  is the growth rate of  $l$  with respect to the concentration of Si interstitials in SiO<sub>2</sub>,  $K_1$  and  $K_2$  are parameters regarding the Si diffusion rate, and  $C_1^f$  is the equilibrium concentration of Si interstitials at the fault. As shown in eq. (1), the OSF growth rate is determined only by the oxide growth rate and the parameters relating to SiO<sub>2</sub> that are independent of the substrate material. Therefore, this OSF growth rate equation may also account for the growth of line-shaped faults in SiC. Accordingly, it was assumed that eq. (1) is applicable to line-shaped faults in SiC. The solid line in Fig. 5 was obtained from eq. (1) with the observed  $dX/dt$  values for the present oxidation conditions. The observed  $l$  values are roughly on the calculated line. Again, it should be noted that all the parameters of eq. (1) used in the calculation are the same values for Si oxidation.<sup>24</sup> Since it has been considered that the SiC oxidation process involves not only Si diffusion but also C diffusion,<sup>11,25-27</sup> the C diffusion may not significantly affect the growth of OSFs.

In conclusion, PL imaging was performed to investigate the effect of thermal oxidation on faults in 4H-SiC epilayers. A comb-shaped BPD array was found to be deformed by thermal oxidation.

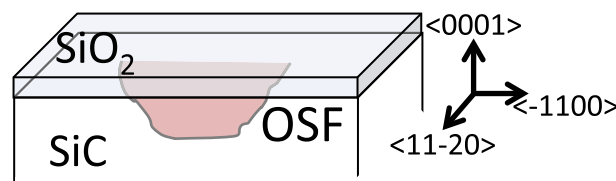


FIG. 6. Schematic illustration of an OSF.

The SF in the vicinity of this BPD array is regarded as a propagated type 1SSF due to its annealing characteristics and shape. Line-shaped faults perpendicular to the off-cut direction were also observed and they were extended more with the oxidation time. In addition, 2SSFs were formed from the line-shaped faults as the starting point by laser irradiation. The line-shaped faults are considered to be OSFs, which are similar to that for Si.

## ACKNOWLEDGMENTS

This work was supported in part by a Grant-in-Aid for Scientific Research from the Japan Society for the Promotion of Science (#15H03967).

- <sup>1</sup> H. Matsunami and T. Kimoto, *Mater. Sci. Eng., R.* **20**, 125 (1997).
- <sup>2</sup> H. Tsuchida, I. Kamata, and M. Nagano, *J. Cryst. Growth* **310**, 757 (2008).
- <sup>3</sup> I. Kamata, X. Zhang, and H. Tsuchida, *Appl. Phys. Lett.* **97**, 172107 (2010).
- <sup>4</sup> G. Feng, J. Suda, and T. Kimoto, *Appl. Phys. Lett.* **92**, 221906 (2008).
- <sup>5</sup> G. Feng, J. Suda, and T. Kimoto, *Appl. Phys. Lett.* **94**, 091910 (2009).
- <sup>6</sup> H. Lendenmann, F. Dahlquist, N. Johansson, R. Soderholm, P. A. Nilsson, J. P. Bergman, and P. Skytt, *Mater. Sci. Forum* **353**, 727 (2001).
- <sup>7</sup> H. Lendenmann, F. Dahlquist, J. P. Bergman, H. Bleichner, and C. Hallin, *Mater. Sci. Forum* **389**, 1259 (2002).
- <sup>8</sup> J. Q. Liu, M. Skowronski, C. Hallin, R. Soderholm, and H. Lendenmann, *Appl. Phys. Lett.* **80**, 749 (2002).
- <sup>9</sup> H. Fujiwara, T. Kimoto, T. Tojo, and H. Matsunami, *Appl. Phys. Lett.* **87**, 051912 (2005).
- <sup>10</sup> K. Nakayama, Y. Sugawara, H. Tsuchida, C. Kimura, and H. Aoki, *Jpn. J. Appl. Phys.* **50**, 04DF04 (2011).
- <sup>11</sup> T. Hiyoshi and T. Kimoto, *Appl. Phys. Express* **2**, 091101 (2009).
- <sup>12</sup> R. S. Okojie, M. Xhang, P. Pirouz, S. Tumakha, G. Jessen, and L. J. Brillson, *Appl. Phys. Lett.* **79**, 3056 (2001).
- <sup>13</sup> H. Yamagata, S. Yagi, Y. Hijikata, and H. Yaguchi, *Appl. Phys. Express* **5**, 051302 (2012).
- <sup>14</sup> M. Nagano, I. Kamata, and H. Tsuchida, *Mater. Sci. Forum* **778–780**, 313 (2014).
- <sup>15</sup> Y. Miyano, S. Yagi, Y. Hijikata, and H. Yaguchi, *Mater. Sci. Forum* **821–823**, 327 (2015).
- <sup>16</sup> R.A. Berechman, S. Chung, G. Chung, E. Sanchez, N.A. Mahadik, R.E. Stahlbush, and M. Skowronski, *J. Cryst. Growth* **338**, 16 (2012).
- <sup>17</sup> T. Miyanagi, H. Tsuchida, I. Kamata, T. Nakamura, K. Nakayama, R. Ishii, and Y. Sugawara, *Appl. Phys. Lett.* **89**, 062104 (2006).
- <sup>18</sup> J. Q. Liu, H. J. Chung, T. Kuhr, Q. Li, and M. Skowronski, *Appl. Phys. Lett.* **80**, 2111 (2002).
- <sup>19</sup> H. J. Chung, J. Q. Liu, and M. Skowronski, *Appl. Phys. Lett.* **81**, 3759 (2002).
- <sup>20</sup> S. I. Maximenko and T. S. Sudarshan, *J. Appl. Phys.* **97**, 074501 (2005).
- <sup>21</sup> T. Yamamoto, Y. Hijikata, H. Yaguchi, and S. Yoshida, *Jpn. J. Appl. Phys.* **47**, 7803 (2008).
- <sup>22</sup> K. Kouda, Y. Hijikata, H. Yaguchi, and S. Yoshida, *J. Appl. Phys.* **112**, 024502 (2012).
- <sup>23</sup> K. Taniguchi, Y. Shibata, and C. Hamaguchi, *J. Appl. Phys.* **65**, 2723 (1989).
- <sup>24</sup> S. T. Dunham and J. D. Plummer, *J. Appl. Phys.* **59**, 2551 (1986).
- <sup>25</sup> Y. Hijikata, H. Yaguchi, and S. Yoshida, *Appl. Phys. Express* **2**, 021203 (2009).
- <sup>26</sup> Y. Hijikata, S. Yagi, H. Yaguchi, and S. Yoshida, in *Physics and Technologies of Silicon Carbide Devices*, edited by Y. Hijikata (InTech, 2013), Chap. 7, p. 181.
- <sup>27</sup> T. Christen, A. Ioannidis, and C. Winkelmann, *J. Appl. Phys.* **117**, 084501 (2015).